Ordered and disordered models of local structure around Ag cations in silver borate glasses based on x-ray absorption near-edge structure spectroscopy

O. Šipr

Institute of Physics, Academy of Sciences of the Czech Republic, Cukrovarnická 10, CZ-162 53 Prague, Czech Republic

G. Dalba

INFM and Dipartimento di Fisica, Università di Trento, Via Sommarive 14, I-38050 Povo (Trento), Italy

F. Rocca

IFN-CNR, Istituto di Fotonica e Nanotecnologie del Consiglio Nazionale delle Ricerche, Sezione "CeFSA" di Trento, Via Sommarive 18, I-38050 Povo (Trento), Italy

The local coordination of Ag cations in silver borate glasses $Ag_2O \cdot nB_2O_3$ has been studied by comparing the experimental x-ray absorption near edge structure (XANES) at the Ag K edge with results of theoretical simulations. We demonstrate that simple models which describe the local structure around Ag with a single geometric configuration cannot be reconciled with experimental XANES spectra. In order to obtain a satisfactory agreement between theory and experiment, it is necessary to include the disorder also at the short range. Structural information is extracted from XANES data using an empirical approach, which is based on the presence of a multiplicity of atomic structural configurations around photoabsorbing atoms. This approach is particularly suited for describing the local environment of atomic species belonging to glass network modifiers.

I. INTRODUCTION

The sensitivity of x-ray absorption near edge structure (XANES) to the local structure of the absorbing site (symmetry, distances, and angles) is generally exploited to quantitatively describe systems characterized by single or few atomic configurations. XANES spectroscopy has allowed the local structural description of compounds in many scientific fields, such as biological samples, solutions, solid-state materials, very diluted systems, surfaces, nanostructured materials, etc.[1] XANES is a particularly well-tailored tool for exploring the local order in multicomponent glasses, thanks to its chemical selectivity and an inherently local nature. The capability of XANES to provide information about short and medium range order has been well recognized and several consistent XANES analysis computer codes are currently used as, for instance, FEFF,[2] FDMNES,[3] and MXAN.[4,5] However, the use of routine best-fit procedures to fit experimental spectra can give rise to unreliable results, when applied to systems where several atomic configurations around the absorbing species are present, as in the case of some glasses.

In this paper we present a study of structural configurations of Ag cations in borate glasses $Ag_2O \cdot nB_2O_3$. Borate glasses are host of widespread optical, electrical, magnetic, and other technologically interesting properties.[6] Silver borate glasses in particular have attracted a lot of attention because of their high ionic conductivity, especially when mixed with AgI. This property makes a basis for their applications in electrochemistry as solid electrolytes.[7] The optimization of such properties requires a good knowledge of the microscopic glassy structure. In particular, a deeper knowledge of the local environment of the moving ions is highly desirable.[8]

The knowledge of their local structure will undoubtedly facilitate the comprehension of the physical properties of these glasses. The local coordination of silver cations has been studied by various spectroscopic and structural techniques both in binary ($Ag_2O \cdot nB_2O_3$) and ternary (i.e., with AgI) glasses.[9–11] Some of the present authors have studied silver borate glasses by x-ray absorption spectroscopy (XAS) in the beginning of 1980, by using the first generation Synchrotron Radiation Sources.[12–15] Those studies were performed at low energies (L edges of silver and iodine) at ADONE (Frascati, Italy), analyzing both XANES and EXAFS (extended x-ray absorption fine structure). While the good energy resolution allowed very accurate XANES spectra comparisons, the results obtained by EXAFS were limited by the short energy range, due to the vicinity of L edges. Only preliminary results were obtained at the high-energy K edge of silver, because of the poor resolution and photon intensity available at ADONE. However, on the basis of all experimental results a structural model for the local coordination of silver and iodine was proposed.[16,17] For binary glasses, XAS experiments identified a mean Ag-O distance of about 2.3 Å and a low coordination number of Ag (around $N \approx 2$). A structural model was suggested with silver bridging between two oxygen atoms in a quasi-linear configuration, as in c-Ag_2O.[13,17]

On the other hand, most recent studies based on reverse Monte Carlo (RMC) analysis of neutron scattering data show evidence of a broader situation, with a distribution of different local sites for Ag cations, having in average a higher coordination number than inferred from EXAFS data.[10] The pair correlation functions $G_{ij}(r)$ for $Ag_2O \cdot nB_2O_3$ simulated by Swenson *et al.*[18] by RMC show that the first peak of the partial $G_{AgO}(r)$ is relatively sharp and symmetrical around

2.4 Å. The coordination number of the first Ag-O peak, N_{Ag-O}, is estimated about 3.3, in good agreement with the value of 3.7 ± 0.5 determined earlier from neutron diffraction experiments.[19] A very broad peak, extending from about 2.5 Å and reaching its maximum value at about 3.1 Å, has been attributed to the $G_{AgB}(r)$ and $G_{AgAg}(r)$ correlations, suggesting a rather disordered coordination between silver and these atomic pairs.[18]

Hence it follows that information available about the local coordination of Ag in binary silver borate glasses is still quite incomplete or, at least, controversial. For this reason, Dalba *et al.*[20] have started a new series of experiments at ESRF (Grenoble, France) using the most powerful Synchrotron radiation source available in Europe. The attention has been focused mainly on the local coordination of AgI in ternary glasses,[21] however, new XANES and EXAFS spectra are now available at the silver K edge of binary glasses as well.

The standard EXAFS analysis of the new data, using a single-shell model for the first coordination shell and c-Ag_2O as experimental reference compound, confirms the previous analysis in terms of the Ag-O distance but appears to be unable to quantify the coordination number unambiguously. In particular, the very low intensity of the first shell Ag-O peak compared with the c-Ag_2O reference spectrum is quite difficult to be interpreted only in terms of a single-shell distorted coordination.[22] Thus, other approaches towards exploiting the available XAS data have to be searched for. One possibility is to employ different methods of EXAFS analysis aiming to search for a model-independent radial distribution function around the absorbing atoms. Work is currently in progress using an algorithm implemented in the EDARDF software package.[23] Another option is to make use of the potential of XANES for structural analysis[5] and to try to use it for gaining more specific (or at least complementary) information on binary silver borate glasses.

There are some good reasons why the XANES can offer a different picture of the geometry around the absorbing site than the more widely employed EXAFS spectroscopy. First, it is more sensitive to multiple-scattering contributions, reflecting thus not only the bond lengths but also the bond angles as well. Second, the chemical type of the atoms around the absorber may affect XANES differently than EXAFS because the energy dependence of the scattering amplitude varies according to the atomic type. And third, XANES is less damped by the disorder, meaning that signals originating from scattering by the second and higher coordination shells are more pronounced in XANES than in EXAFS [recall that in a simple EXAFS formula, the damping rises exponentially with energy due to the $\exp(-2\sigma^2 k^2)$ term,[24] with σ being the Debye-Waller factor and k the photoelectron wave vector]. This becomes especially important when studying systems with a strong static disorder—which is the case of glasses.

XANES spectroscopy was applied for several structural studies of disordered systems in the past. The method one usually employs is to calculate the theoretical spectra for various models of the nearest neighborhood around the photoabsorbing atom and to look for the best agreement between theory and experiment. In some cases, it was enough to take just a single geometric configuration (or only a few of them) into account in order to reproduce the experimental spectrum successfully; typically, the structures of these configurations are based on structures of crystalline counterparts of the amorphous systems. The materials in which this approach apparently works include amorphous germanium,[25] titanosilicates[26] and aluminosilicates,[27] or amorphous $Al_{90}Fe_xCe_{10-x}$ alloys.[28] One can assume that these systems maintain a well-defined "semiordered" structure in the short and sometimes even medium length scale. On the other hand, for other compounds a good agreement with experiment was achieved only if the theoretical spectrum was formed by making an average of spectra calculated for a large number (~ 100) of different geometric configurations. This is the case of Fe-B, Ni-B, and Fe-Zr amorphous alloys[29–31] or of aqueous solution of $Cr(H_2O)_6^{3+}$ (Ref. 32). Different results were found for amorphous SiO_2—some works indicate that a single SiO_4 cluster is sufficient for a proper reproduction of XANES,[33,34] while use of larger clusters and accounting for the site disorder was found to be important in another study.[35]

It emerges thus that there might be in fact two categories of amorphous systems, according to the way in which their local structure has to be described. The first category is formed by systems in which a semiordered short-range structure around atoms of a given chemical type can be identified: it means that it can be (at least approximately) described by a single geometric configuration. The compounds investigated in Refs. 25–28 may serve as examples. The disorder is significant only at the medium or long range in these systems and it can be effectively included in XANES calculation simply by restricting the size of the cluster involved. We call this procedure a "single-configuration approach." Systems in which semirigid local structural units cannot be identified (even at the short range) fall into the second category. The local structure around atoms in such systems can only be described as a superposition of many geometric configurations. In order to account for this kind of disorder, one has to calculate the XANES spectrum as an explicit average of spectra calculated for a large number of individual geometric configurations, as done in Ref. 29–31. The whole set of such configurations can be then regarded as a structural model for this type of systems. We call it a "multiconfiguration" approach in this work.

The purpose of this paper therefore is to look on the $Ag_2O \cdot nB_2O_3$ glasses from this viewpoint, to decide into which of the two categories these glasses belong and to find out as much about the local structure around Ag atoms as possible. In the beginning (Sec. II), the strategy we use for extracting structural data from XANES of silver borate glasses is reviewed. We argue that even if a single-configuration approach fails, useful information can be obtained by observing how the calculated spectra depend on some basic structural parameters. Then we present our experimental results (Sec. III) and describe briefly the method we use for calculating XANES (Sec. IV). After demonstrating that the measured spectra cannot be reproduced by relying on single geometric configurations (Sec. V A), we turn to the second

approach and try to reproduce the experiment by averaging over many configurations, generated along certain rules (Sec. V B). By exploring the trends in the theoretical spectra of both the semiordered and randomized models upon varying certain structural characteristics we obtain some geometrical conditions which acceptable structural models ought to obey. Some general conclusions concerning the formation of distinct features in XANES spectra of glasses are drawn and the applicability of our method of analyzing XANES of amorphous systems is assessed afterwards (Sec. VI).

II. EXTRACTING STRUCTURAL INFORMATION FROM XANES OF GLASSES

Despite continuous studies of the relationship between XANES and the geometry around the absorbing atom,[36–41] there is no simple prescription how to extract from experiment the desired structural information. Unlike in EXAFS, no direct inversion of the measured data is possible. This is partly due to the physical complexity of the processes underlying the x-ray absorption spectra in the near-edge region (multiple scattering), but also to the still insufficient accuracy and reliability of routine XANES calculations (stemming mainly from approximate treatment of core hole effects and from muffin-tin approximation). Therefore one has to look for new approaches, which ought to be both informative and robust.

As already mentioned, the most immediate method is to compare the experimental spectrum with spectra calculated for a number of trial structures and to search for the best fit. The weak point of this approach is that, given the deficiencies of current XANES calculations, one can be easily led to false conclusions: a correct guess of the structure may be actually rejected by the algorithm if it results in a poor agreement with experiment due to the defects of the theory itself. If the ''rejection threshold'' is raised correspondingly, the task of optimizing too many structural parameters may become ambiguous. Despite this principal difficulty, several promising procedures for analyzing XANES of glasses were developed recently. An attempt to circumvent the defects of the XANES theory by a suitably chosen weighting function was undertaken by Benfatto and co-workers.[4] A survey of distribution of prepeak heights and positions in a number of Ti containing compounds was used by Farges et al.[38,42] to obtain information about coordination of Ti in titanium silicate glasses and melts. The information that can be obtained in this way is restricted but at the same time solid and credible. On the contrary, the quantitative EXAFS-like determination of interatomic distances and coordination numbers through a Fourier filtration of XANES signal, proposed by Bugaev et al.,[43] relies on certain disputable assumptions about the significance of various contributions to the XANES spectrum. The potential and universality of these and other approaches still has to be fully explored.

The procedures outlined above need a considerable amount of knowledge about the structure to be available beforehand. Moreover, the best-fit technique and related procedures would probably fail for systems whose structure cannot be described by a single geometric configuration, as the number of structural parameters to be fitted would grossly exceed a tractable maximum of ten or so.[5] As the current knowledge of the local structure around Ag cations in $Ag_2O \cdot nB_2O_3$ glasses is quite a limited one and (as we will show later) the single-configuration description does not work well for these materials, a different strategy is followed in this work. Its core rests in resigning on finding detailed and specific information about all the coordinations of Ag atoms which may be present in the material. On the contrary, the efforts are concentrated on searching for some general structural conditions which the *statistically averaged* neighborhoods of Ag atoms have to comply with, so that significant features of the experimental spectrum are reproduced. At the beginning of our procedure, we select a reasonable starting model from few simple trial structures (in this point, at least some primordial knowledge from earlier EXAFS and neutron scattering analysis is indispensable). Then we progressively introduce the disorder and observe the trends of the site-averaged spectra as a function of changes of few structural parameters (such as average coordination number or first-shell distance). By observing which features of our test models are essential for achieving an acceptable agreement between theory and experiment, we can decide which structural models are most plausible. Provided that similar conclusions about some basic structural characteristics are reached under various conditions, one can have confidence in their reliability. So this approach represents a trade off between specificity and robustness. It can be seen as a merge between the approaches of Farges et al.[38,42] and of Kizler et al.[29–31] It does not lead to a simple and unique solution to the problem of finding the actual structure of glasses, however, it may provide a relevant structural information in cases where description of local structure around specific atoms in terms of a single geometric configuration fails.

Apart from providing information about the structure of silver borate glasses, this study may elucidate general mechanisms of formation of XANES spectral features. A special attention will be devoted to investigate the effects of a gradually introduced disorder.

III. EXPERIMENT

The samples of binary silver borate glasses $Ag_2O \cdot nB_2O_3$ were prepared by standard melt quenching procedures and tested for absence of crystallinity in our laboratory. Different chemical compositions were prepared, ranging from silver diborate to silver octaborate. XAS measurements were carried out in Grenoble at the beamline BM8-Gilda Crg of ESRF, in the high-energy configuration, without focusing. We used a double Si(311) crystal monochromator obtaining an energy resolution of about 2.5 eV, which is well bellow the Ag $1s$ core hole lifetime.[44]

The normalized Ag K edge XANES spectra for diborate ($n=2$), triborate ($n=3$), tetraborate ($n=4$), hexaborate ($n=6$), and octaborate ($n=8$) glasses are presented in the Fig. 1, together with the spectrum of crystalline silver oxide Ag_2O for comparison. The curves have been aligned horizontally with respect to their first inflection point, the origin of the energy scale is arbitrary.
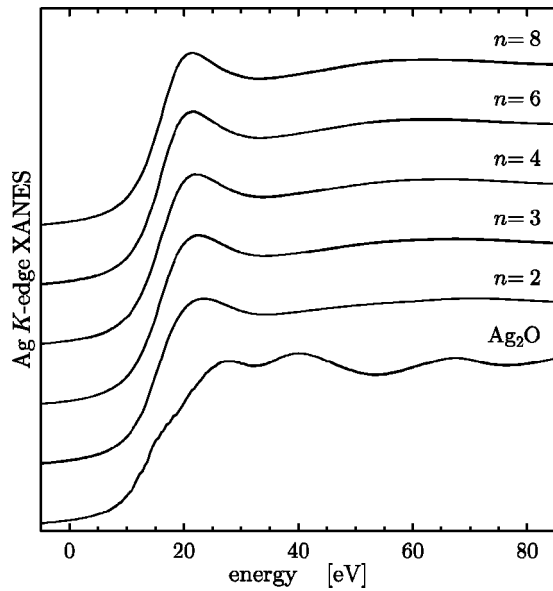
FIG. 1. Experimental Ag K edge XANES spectra of silver borate glasses $Ag_2O \cdot nB_2O_3$. Each curve is identified by the B_2O_3 content n. Spectrum of crystalline silver oxide Ag_2O is included for comparison. The origin of the energy scale is arbitrary.

As in the case of Ag L_1 and L_3 edges (cf. Ref. 12), the spectra of glasses of different compositions look quite similar to each other. Their dominant features comprise a well-defined and relatively sharp first peak at 21–24 eV followed by a broad second maximum around 60–70 eV. A general systematic trend can be observed if the $Ag_2O \cdot nB_2O_3$ composition is varied: the intensity of the first peak slightly but steadily increases with n and the energy separation of the two main peaks decreases (from 46 eV for $Ag_2O \cdot 2B_2O_3$ to 41 eV for $Ag_2O \cdot 8B_2O_3$). Apart from that, the spectrum of $Ag_2O \cdot 2B_2O_3$ exhibits a weak but still well-defined shoulder at the low-energy side of the second peak (at ~ 53 eV). The Ag K edge spectra of $Ag_2O \cdot nB_2O_3$ glasses look quite similar to the Ag L_1 edge spectra within the whole range for which the L_1 spectra are available,[12] indicating that no important spectral features have been lost by the relatively large $1s$ core hole lifetime broadening.

The two main peaks present the key features which have to be reproduced by any acceptable XANES calculation. Because of the overall similarity of the experimental spectra for all n and because our structural models will necessarily be only approximate, we are not going to distinguish specifically between individual $Ag_2O \cdot nB_2O_3$ compositions in the following analysis, unless it is stated otherwise.

IV. THEORY

The spectra were calculated within the real-space multiple-scattering technique,[45] which is particularly suitable for studying amorphous systems as it does not rely on translational periodicity (it concerns just a finite cluster of atoms). We used the RSMS code, which is an amended descendant of the ICXANES code[46] and is maintained by our group.[47] Full

multiple scattering among all the atoms of our model clusters was included via a matrix inversion.

Non-self-consistent muffin-tin potentials constructed according to the Mattheiss prescription (superposition of potentials and charge densities of isolated atoms) were employed. Although self-consistent potentials could be, in principle, obtained from cluster calculations,[2,48,49] we refrained from their use because the benefit would hardly compensate for the extra demand on computing (XANES of several thousand of geometric configurations had to be calculated). We are led to this conclusion by earlier studies which showed that self-consistency in potentials does not have a profound effect on the calculated spectra of Ag_2O.[49] Moreover, when constructing accurate self-consistent potentials for the model clusters, one ought to account for the influence of even more distant atoms whose positions are uncertain and the scattering potential thus inherently contains some errors (especially as concern the long range Coulombic contributions). As a whole, it is very likely that errors caused by deviations of structural models from the true geometry will be much more significant than errors introduced by inadequacy of the scattering potential.[5]

The calculated spectra display no pronounced core hole effect; just the intensity of the first peak may increase by less than 10%. This observation is in accord with our earlier study of Ag_2O (Ref. 49). As we checked explicitly that the results of our analysis do not depend on the inclusion or neglect of the core hole, we display here for simplicity the spectral curves calculated for the potential which neglects it (i.e., the ground-state potential).

The exchange-correlation potential of Ceperley and Adler[50] was used for atomic calculations of the occupied states. In constructing the Mattheiss potential appropriate for unoccupied states, the energy-independent $X\alpha$ potential with the Kohn-Sham value of $\alpha = 0.66$ was used.[51] We do not employ energy-dependent exchange-correlation potential here as no universal recipe how to select its optimal form for a particular case has been known so far.[52,53] In any case its choice would hardly affect our assessment of various structural models because we are concerned primarily with the very existence or nonexistence of main spectral features or with the trends of these features upon geometry variations.

For calculating spectra of models derived from the structure of silver borate crystals (Sec. V A), the potential obtained for the corresponding crystal structure is taken. For studying more general models based on averaging over many geometric configurations (in Sec. V B), the same potential for all the models is used, in order to expose only the net effect of the changes in the geometry. This "universal potential" is taken over from silver orthoborate crystal ($3Ag_2O \cdot B_2O_3$) for convenience, because all the atoms are in quite symmetric and compact coordinations in this compound, meaning that the superposed atomic charge densities would not change dramatically if the atomic positions are changed. Moreover, there is just one crystallographic site for each chemical species in this compound, which simplifies the matters formally. We checked that this particular choice of potential is not crucial for our study: very similar theoretical curves were obtained for a number of other potentials ob-
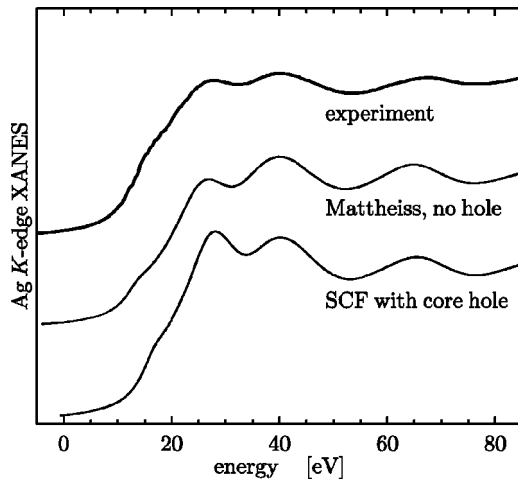
FIG. 2. Experimental (upper curve) and theoretical (middle and lower curves) Ag K edge XANES of c-Ag_2O. The theoretical spectra correspond to a non-self-consistent potential with the core hole ignored (middle curve) and to a self-consistent potential with the $1s$ core hole included (lowermost curve).

tained for other plausible geometric arrangements (either silver borate crystals or artificial cubic structures). The fact that the calculated XANES of model borate structures depends only weakly on the scattering potential serves as yet another hint that it is not necessary to use self-consistent potentials in this study. Also, it indicates that the chemical state of the Ag atoms affects the XANES of $Ag_2O \cdot nB_2O_3$ glasses significantly less than the geometric arrangement of its neighborhood. In fact robustness of the calculated spectra with respect to finer effects of the scattering potential is an indispensable prerequisite for the kind of analysis we are doing in this work: one could not hope to find reliable conclusions about the structure of glasses, if the calculated spectrum depended crucially on tiny variations of the scattering potential induced by changes of the model geometry.

Raw theoretical data were convoluted by a Lorentzian curve with an energy-dependent width $\Gamma(E)$ set according to the *ansatz* $\Gamma(E) = 6.0$ eV for $E \lesssim 10$ eV and $\Gamma(E) = 6.0 + 0.2 \times (E - 10.0)$ eV for $E > 10$ eV. This formula was chosen in analogy with other works,[4,54] and leads to a reasonable shape of the Ag_2O spectrum (Fig. 2). Its constant part may be viewed as accounting primarily for the core hole lifetime[44] while the energy dependent part mimics intrinsic and extrinsic inelastic losses.[5,55] The agreement between theory and experiment could certainly be improved by an *ad hoc* optimization of the (generally unknown) smearing function $\Gamma(E)$, however, we did not do that as such an improvement would not in fact reflect a better guess of the geometric structure. In any case we verified that choosing a different formula for $\Gamma(E)$ does not change our conclusions about the structure of $Ag_2O \cdot nB_2O_3$ glasses.

The alignment of the theoretical spectra in energy is such that the best overall agreement between theory and experiment is achieved. The vertical scale of the calculated curves is uniform throughout all this paper and was set so that it matches the experimental curves.

The accuracy of our calculations can be inferred from Fig.

2, where the Ag K edge XANES of Ag_2O calculated for a 119-atoms cluster is compared with experiment. Results for two types of scattering potential are shown: a non-self-consistent potential with the core hole ignored (middle curve in Fig. 2) and a self-consistent potential with the $1s$ core hole included (lowermost curve). Both potentials reproduce the significant characteristics of experimental spectrum at their correct energy positions. The precise form of the scattering potential does not have a profound effect on the calculated spectrum; the most potential-sensitive feature appears to be the intensity of the first spectral peak at ~ 26 eV. Most of the difference between the two theoretical spectra of Fig. 2 originates from the self-consistency (about 60–70 %), with the core effect playing only a secondary role (30–40 %). A similar comparison for $Ag_2O \cdot nB_2O_3$ crystals could not have been made as there are no experimental spectra available for these systems, to the best of our knowledge. We conclude that the overall good agreement between the theory and experiment in the case of Ag_2O, which is one of the parent compounds of $Ag_2O \cdot nB_2O_3$ glasses, indicates that our theoretical framework can be used as a basis for this study.

V. RESULTS

A. Single-configuration models

Crystalline analogs present a natural starting point for modeling the local order in glasses. Structures of silver orthoborate $3Ag_2O \cdot B_2O_3$, metaborate $Ag_2O \cdot B_2O_3$, and tetraborate $Ag_2O \cdot 4B_2O_3$ crystals can be found in the literature.[56–58] While the structure of silver orthoborate crystal is relatively simple, the remaining two crystal structures are quite complex—they are formed by a network of B-O chains, interconnected by Ag atoms. Although there is just one silver site in $3Ag_2O \cdot B_2O_3$, there are five nonequivalent silver positions in $Ag_2O \cdot B_2O_3$ and two in $Ag_2O \cdot 4B_2O_3$. We label those sites Ag-1, . . . , Ag-5. The nearest neighbors of silvers are always oxygens (the least three of them). Schematic diagrams of the crystal structures can be found in Refs. 56–58.

We calculated the K edge spectra around each of the Ag sites in the three silver borate crystals, for several cluster sizes (10–60 atoms). None of the calculated spectra exhibits the characteristic features of experimental XANES of silver borate glasses with a sufficient accuracy: either the first maximum is too low and too broad, or the separation between the first and the second peak is too small, or both. The closest resemblance between the theoretical XANES of crystals and experimental XANES of glasses was obtained for the Ag-5 site in silver metaborate $Ag_2O \cdot B_2O_3$ and the Ag-2 site in silver tetraborate $Ag_2O \cdot 4B_2O_3$. These spectra are shown in Fig. 3 by dashed lines: the first to the third graphs from the bottom stand for $Ag_2O \cdot B_2O_3$, the fourth to the sixth graphs represent $Ag_2O \cdot 4B_2O_3$ (note that the dashed curves are identical inside each of the triads). All the theoretical spectra presented in Fig. 3 were obtained for middle-sized clusters containing between 20 to 31 atoms.

When performing a "standard" best-fit geometry optimization, one has to quantify the differences between various spectral curves. Although we do not employ the best-fit pro-
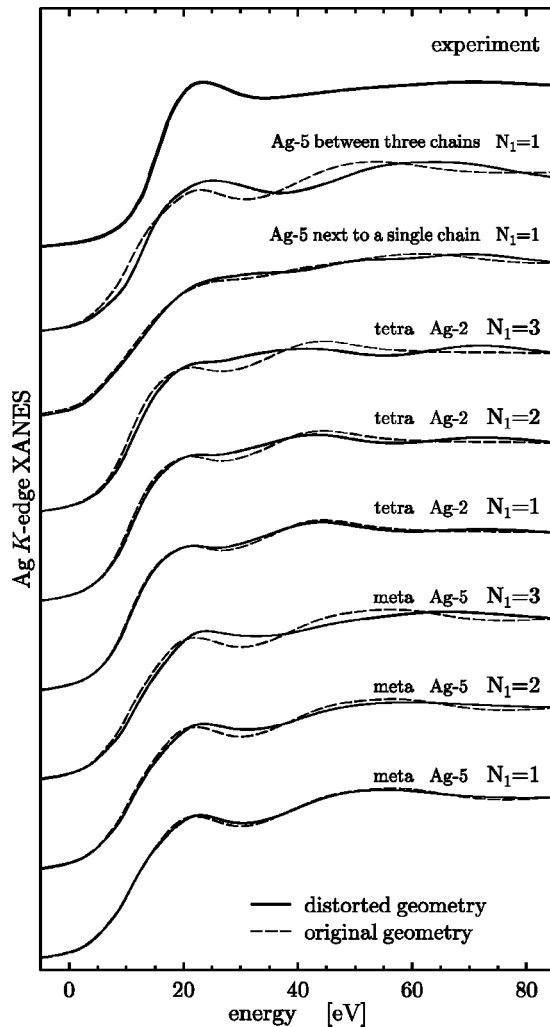
FIG. 3. Theoretical Ag K edge spectra for structural models derived from silver borate crystals. Full lines in the six lowermost graphs correspond to models obtained by moving the N_1 nearest oxygens radially so that their distance from the central Ag is 2.27 Å. The second and the third from the top graphs correspond to moving the Ag atom perpendicularly to the direction of B-O chains (see the text). Spectra calculated for clusters cut off nondeformed crystals are drawn by dashed lines. Experimental spectrum of $Ag_2O \cdot 2B_2O_3$ glass is shown in the top graph for comparison. A quantitative evaluation of the displayed spectra is summarized in Tables I and II.

cedure in this study, it might still be instructive to present some quantitative assessment of the agreement between theoretical spectra for model structures and the experimental spectra of glasses. In EXAFS analysis it is common to rely on the R^2 factor, which is defined as

$$R^2 = 100 \frac{\int dE[Y_{the}(E) - Y_{exp}(E)]^2}{\int dE[Y_{exp}(E)]^2},$$

where Y_{the} and Y_{exp} are the theoretical and experimental spectral intensities, respectively. Another quantitative mea-

sure might be the difference Δ_{peaks} between the theoretical and experimental energy separations of the two main spectral peaks (in experiment, this separation is 46.4 eV for $Ag_2O \cdot 2B_2O_3$ and 44.0 eV for $Ag_2O \cdot 4B_2O_3$). However, the R^2 factor is tailored for comparing oscillating EXAFS-like functions and the peaks separation Δ_{peaks} accounts for only one, though important, feature of the spectral curves. These quantities are, therefore, only of a lesser relevance to our situation; a less rigorous but more comprehensive visual inspection of the XANES curves still appears to be more appropriate in this case as it can account for trends and features, the quantification of which cannot be automated in a straightforward way. In order to connect our work to other studies dealing with similar topic, we present the R^2 and Δ_{peaks} values for some instructive cases nevertheless. However, one has to bear in mind that the minimization of the R^2 factor is not a sufficient condition to select the more probable structural models for the problem we are studying. For the spectra of undistorted crystals displayed by the two lowermost triads of dashed lines in Fig. 3, the corresponding R^2 and Δ_{peaks} values are summarized in the two bottom lines of Table I.

The fact that theoretical XANES of silver borate crystals does not satisfactorily reproduce experimental spectra of glasses is not so surprising—some changes of the local geometry around Ag atoms had to be anticipated. As a next step, we explore several models derived from the crystals by deforming their structure in a suitable way. We start with either contracting or expanding radially the distances of the N_1 nearest oxygens, so that the nearest Ag-O distance would be either 2.02 or 2.27 Å (in agreement with earlier EXAFS studies),[17] while keeping the remaining atoms in their original positions. We found that although these changes sometimes lead to spectra which resemble the experimental XANES of glasses more closely than in the case of undistorted crystals, the improvement is yet not sufficient enough to convince that these amended models could serve as a good description of silver borate glasses. Representative results for the Ag-5 site in $Ag_2O \cdot B_2O_3$ and for the Ag-2 site in $Ag_2O \cdot 4B_2O_3$ are displayed by full lines in the six lowermost graphs of Fig. 3 (we put either $N_1 = 1$, 2, or 3 oxygens at the distance of 2.27 Å from the central Ag, as indicated by the labeling). A quantitative assessment of these spectra is shown in Table II (the third to the last lines). Other silver sites and nearest Ag-O distances were explored as well; none of the combinations leads to an essentially better picture.

Yet another approach to generating new trial structures is to keep the individual B-O chains rigid while moving them either closer to or away from each other, so that the distances between the interconnecting Ag atoms and their nearest neighbors can be varied. We focused specifically on the chains which form silver metaborate crystal, because these served as a starting point for an earlier structural analysis of borate glasses based on x-ray diffraction.[11] As one can concentrate on any of the nonequivalent silver sites and include various numbers of B-O chains, a large number of models can be created in this way. We investigated the case of a single B-O chain with silver atoms attached to it and of three B-O chains running in parallel with each other, with silver

TABLE I. The R^2 factor and the difference between main peaks separations Δ_{peaks} for theoretical spectra of undistorted silver borate crystals (displayed with dashed lines in Fig. 3) and experimental spectra of silver borate glasses. The first column identifies the structural model (see the text for more details), the second and third columns concern the comparison with experimental spectrum of $Ag_2O \cdot 2B_2O_3$ glass, the fourth and fifth columns represent the same for $Ag_2O \cdot 4B_2O_3$ glass.

| Model | $Ag_2O \cdot 2B_2O_3$ | | $Ag_2O \cdot 4B_2O_3$ | |
	R^2	Δ_{peaks} (eV)	R^2	Δ_{peaks} (eV)
Between 3 chains	0.88	-15.9	1.47	-13.4
Next to 1 chain	2.88	-11.4	4.24	-9.0
Tetraborate	27.84	-16.9	31.81	-14.4
Metaborate	0.72	-11.9	1.18	-9.4

atoms between them. The nearest Ag-O distance was tuned by moving the B-O chains in directions perpendicular to them. None of these models leads to a good agreement between its theoretical XANES and the experimental spectra of the glasses. Therefore only two illustrative examples are displayed in the second and third from the top graphs of Fig. 3 (cf. also first two lines in Table II). These models are formed by either one or three B-O chains, with the smallest Ag-O distance (of 2.27 Å) at the Ag-5 site. Note that the corresponding calculated spectra of undistorted crystals (drawn by dashed lines) differ from analogous curves in the three bottom graphs of Fig. 3, because the clusters have now been cut from the system defined by B-O chain(s) only and not from the full crystal (meaning that spheres of identical radii ascribed around analogous silver sites do not contain identical numbers of atoms in the "crystalline" and "chain" models). The R^2 and Δ_{peaks} values for the undistorted geometries cut off in this way are shown in the first two lines of Table I.

As a whole, our results indicate that silver borate *crystals* are not a good starting point for modeling XANES of silver borate glasses. We checked that using crystal structures of other chemically related borates, in particular lithium diborate $Li_2O \cdot 2B_2O_3$ (Ref. 59) and α and β natrium triborate $Na_2O \cdot 2B_2O_3$ (Ref. 60) and substituting Ag for the cations does not improve this situation. It appears that there is no single configuration dominating the local structure around Ag in silver borate glasses. Consequently, instead of continuing the attempts to nail down *the* correct local structure, we

are going to switch to the multiconfiguration approach and focus on finding some general properties which the local structure should display, without necessarily going into particularities.

B. Averaging over many configurations

1. XANES of generic polyhedra

In order to find a reasonable starting point, we concentrate on generic polyhedra simulating just the nearest Ag neighborhood and explore the way the calculated XANES is affected by their choice. We consider one silver atom surrounded by few oxygens at the distance of 2.27 Å (following EXAFS results of Rocca *et al.*).[17] The number of nearest oxygens ranges from 2 to 8, and the atoms are deployed in such a way that generic shapes, such as square or tetrahedron etc. are created. Selected results of XANES simulation are shown in Fig. 4. The crucial task appears to be the reproduction of the first peak at ~ 22 eV. In most cases, this peak is too broad and too low. The eight-oxygen model, with cubic ordering resembling the nearest neighborhood in a bcc or CsCl crystal structure, appears to be the most plausible of all the polyhedra we explored.

The natural concern is what happens if more distant atoms are included. To check this, we associated with each of the generic polyhedrons a set of hundred clusters created by appending the polyhedron oxygens with randomly oriented BO_m units ($m = 1, 2, 3$) cut from the B-O chains which form

TABLE II. The R^2 factor and the difference between theoretical and experimental main peaks separations for structural models obtained via distorting silver borate crystal structures. The corresponding spectra are displayed with full lines in Fig. 3.

| Model | $Ag_2O \cdot 2B_2O_3$ | | $Ag_2O \cdot 4B_2O_3$ | |
	R^2	Δ_{peaks} (eV)	R^2	Δ_{peaks} (eV)
Between 3 chains	1.12	-7.8	2.08	-5.4
Next to 1 chain	9.13	-12.4	11.41	-9.9
Tetraborate, $N_1 = 3$	20.52	-16.3	23.94	-13.9
Tetraborate, $N_1 = 2$	24.63	-17.1	28.26	-14.6
Tetraborate, $N_1 = 1$	27.12	-18.0	31.06	-15.5
Metaborate, $N_1 = 3$	0.64	-4.4	1.35	-2.0
Metaborate, $N_1 = 2$	0.60	-10.1	1.24	-7.7
Metaborate, $N_1 = 1$	0.70	-14.1	1.28	-11.6
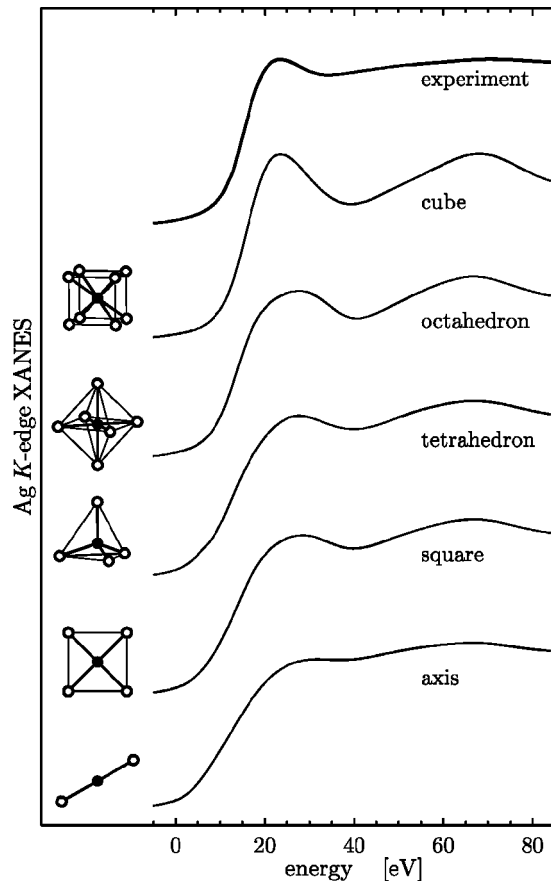
FIG. 4. Theoretical Ag K edge spectra for five generic Ag-centered polyhedra. Each spectrum is identified by the name and schematical diagram of the respective polyhedron (full circle stands for silver, open circles stand for oxygens). Experimental spectrum of $Ag_2O \cdot 2B_2O_3$ glass is included for comparison.

the silver metaborate crystal. The Ag K edge XANES of such a generalized polyhedron model was calculated as an average over spectra of all the clusters belonging to the associated set. We found that although some of the individual clusters give rise to spectra which are significantly different from spectra of bare polyhedrons, the *averaged spectra* of polyhedrons with BO_m appendices are very similar to spectra of polyhedrons without the appendices (hence we do not show them here). So the overall picture offered by Fig. 4 does not change even if some more distant atoms are added in a random way.

We conclude this section be observing that the eight-atoms polyhedron seems to be the most promising candidate for a further refinement of the local structure of $Ag_2O \cdot nB_2O_3$ glasses around Ag and, therefore, we concentrate solely on this model and elaborate it more deeply in the following. We will see in the end that restricting ourselves to this coordination does not harm the generality of our conclusions.

2. Trends in semiordered models

The simple cubic model is obviously too symmetric and ordered to stand as a realistic description of silver borate
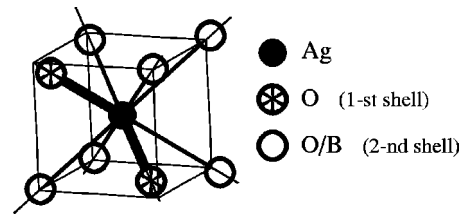
FIG. 5. A schematic diagram of a cube-based model of the local structure around Ag. Positions of the central Ag and of the first-shell oxygens (marked by crosses and thicker bonds) remain unchanged through all the configurations belonging to a particular set, while radial distances and chemical types of the second-shell atoms (marked by empty circles and thinner bonds) differ from configuration to configuration.

glasses. A more realistic model ought to consider that the silver-neighboring atoms will have various radial distances and chemical types. The disorder ought to be incorporated in some way as well. So we construct in this section a more general cube-based semiordered model and explore how the theoretical XANES changes if some of its structural characteristics are varied.

Each structural model we investigate here is represented by a set of individual configurations (clusters), as depicted schematically in Fig. 5. Every cluster consists of a central Ag and of eight "corner" atoms positioned somewhere on the cube body diagonals (i.e., not necessarily at the cube vertices themselves). These eight corner atoms are split into two groups. The nearest N_1 atoms form the "first shell": they are always oxygens and all of them are at the same distance R_1 from the central Ag. The remaining $(8-N_1)$ corner atoms form the "second shell." We assume that K_B of these atoms are borons and the rest of them are oxygens. This second shell is radially blurred: every atom has a different radial distance than any other of them so that these distances cover the interval 2.5–3.0 Å with an equidistant step (meaning that if there are, e.g., five atoms in the second shell, their radial distances will be 2.5, 2.625, 2.75, 2.875, and 3.0 Å). These requirements allow for a large number of distinct geometric configurations with a common first-shell geometry and a fixed number of borons K_B, because we do not specify in which order the radial distances of the second-shell atoms ought to be distributed among the predefined Ag-(O,B) bond directions. We sort these configurations in such a way so that all configurations which share the same positions of the first-shell atoms and thus differ only through arrangement of the second-shell atoms belong to the same set, forming thus a structural model. As a partial disorder is introduced in this way, we call these models "semiordered."

In this work we consider models with the first-shell coordination numbers $N_1 = 2$, 3, or 4, with the first-shell distances $R_1 = 2.0$, 2.2, or 2.4 Å and with either $K_B = 0$, 2, or 4 borons in each cluster. The values of N_1, R_1, and K_B do not yet determine the model uniquely, as the first-shell atoms can still be distributed among the available bond directions in more nonequivalent ways. It can be verified straightforwardly that there are three first-shell geometries for $N_1 = 2,3$ and six first-shell geometries for $N_1 = 4$, so we explore $3 \times 3 \times (3+3+6) = 108$ structural models altogether.
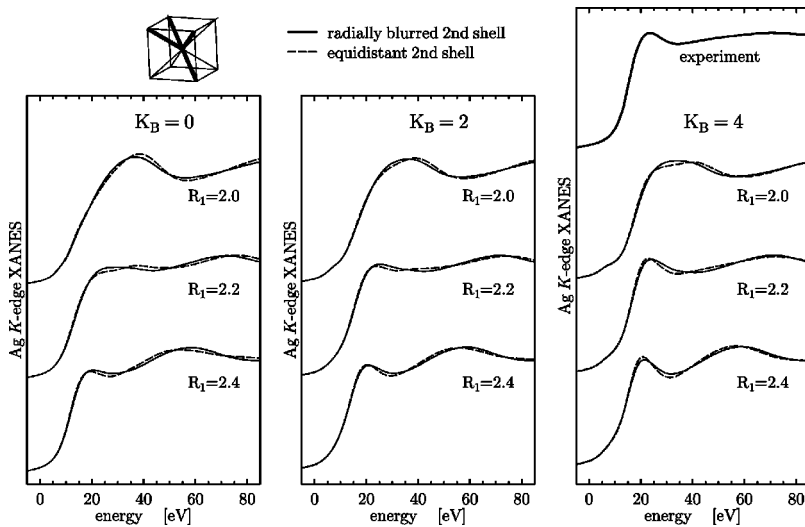
FIG. 6. Configurationally averaged XANES spectra for structural models with $N_1 = 4$ oxygens in the first shell. The arrangement of the first-shell atoms is indicated by the inset above the left panel (first-shell bond directions are shown via thick lines). The number of boron atoms in the second shell K_B varies from zero (left panel) to two (middle panel) to four (right panel), the distance between the first-shell O atoms and the central Ag varies from $R_1 = 2.0$ Å (uppermost graphs) to $R_1 = 2.2$ Å (middle graphs) to $R_1 = 2.4$ Å (lowermost graphs). A corresponding XANES for an equidistant second shell [with all its $(8-N_1)$ atoms at 2.75 Å] is displayed by a dashed curve for each model. Experimental spectrum of $Ag_2O \cdot 2B_2O_3$ glass is shown at the top of the right panel.

The number of configurations associated with each model depends on N_1, K_B, and on the first-shell geometry and varies from just a single configuration (for $N_1 = 4$, $K_B = 0$ or 4, and a tetrahedral arrangement of the first-shell atoms) to 2700 configurations (for $N_1 = 2$, $K_B = 2$ or 4, and the first-shell oxygens located on the same side of the basic cube).

For each of these models, the corresponding Ag K edge XANES was calculated as an average of spectra of all the configurations associated with it. Three fundamental trends are in the focus of our analysis, namely, how does the configurationally averaged XANES change if we vary the number of first-shell oxygens N_1, if we vary the first-shell distance R_1, and if we vary the total number of borons K_B. Apart from that, the effect of radial blurring of the second shell is investigated by comparing the results obtained for the broad distribution of Ag-(O,B) distances as realized by our models with the results obtained for an "equidistant" second shell [with all the $(8-N_1)$ atoms at 2.75 Å]. The plausibility of structural models was judged according to their ability to reproduce the essential features of experimental XANES (a relatively sharp first maximum followed by a second flat peak separated by $\sim$41–47 eV). The "acid test" appears to be the very existence of the first maximum.

Figure 6 shows theoretical spectra for all structural models allowed by $N_1 = 4$ oxygens in the first shell arranged in the way shown schematically by the inset. This plot exposes the evolution of the averaged spectra if R_1 and/or K_B are being varied. One can also see the effect of radial blurring of the second shell because the spectra of corresponding models with equidistant second shells are shown as well (with dashed lines). It follows from Fig. 6 that the best agreement between theory and experiment is obtained for $R_1 = 2.2$ Å. The shortest Ag-O distance of all we tested, $R_1 = 2.0$ Å, leads to quite unsatisfactory XANES curves. Substituting some second-shell oxygens with borons improves the results, with $K_B = 4$ borons in the cluster leading to a slightly better agreement with experiment than in the case of $K_B = 2$. Blurring the second-shell distances over the whole 2.5–3.0 Å interval smears out some redundant oscillations which appear in the equidistant case, especially in the region between the two main peaks (these superfluous oscillations would be

even more evident if a smaller final-state Lorentzian broadening was employed). It also leads to a slight increase of the energy separation between both peaks, improving thus agreement with experiment.

A picture very similar to that offered by Fig. 6 would be obtained if we constructed analogous plots for other numbers N_1 of the first-shell atoms. We do not show the remaining results here in order not to overload the paper with too many graphs. Instead, we focus specifically on the dependence of the calculated XANES on N_1. Each of the three graphs in Fig. 7 illustrates this N_1 dependence for a different setting of the remaining structural characteristics (i.e., R_1 and K_B). The geometric arrangement of the first-shell atoms is shown by insets in the legend. It can be seen that increasing the
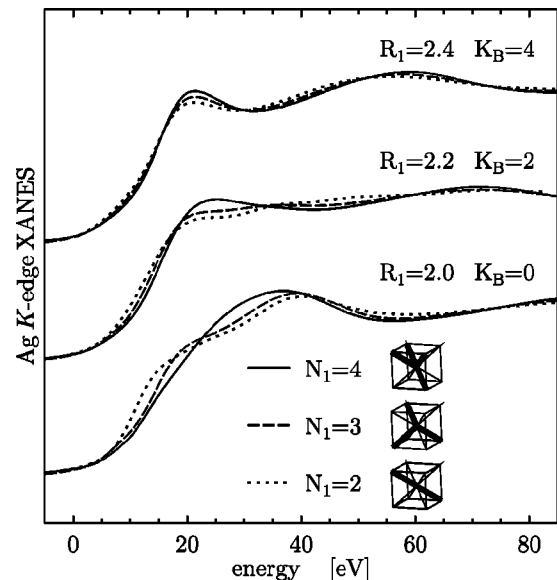
FIG. 7. Configurationally averaged XANES spectra for structural models with $N_1 = 2$ (dotted lines), $N_1 = 3$ (dashed lines), and $N_1 = 4$ (full lines) first-shell atoms. The first-shell distance R_1 and the number of borons K_B remain fixed inside each of the triads of curves and are written above each of them. The geometric arrangements of the first-shell atoms are shown schematically in the legend.
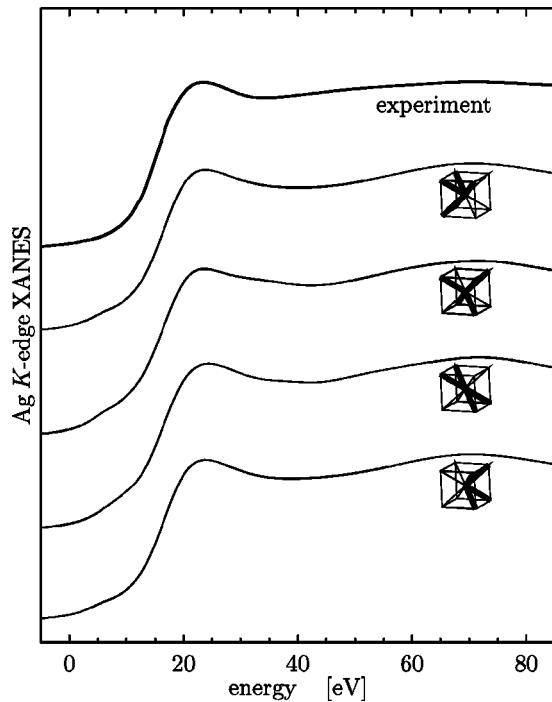
FIG. 8. Configurationally averaged XANES spectra for structural models with identical $N_1 = 4$, $R_1 = 2.2$ Å, and $K_B = 4$ but differing by geometric arrangements of the first-shell atoms. Experimental spectrum of $Ag_2O \cdot 2B_2O_3$ glass is shown at the top.

number of first-shell oxygens N_1 improves the agreement between theory and experiment. Curves with $N_1 = 4$ perform better than curves with $N_1 = 2$ or $N_1 = 3$, provided that other parameters are identical.

It remains to explore how does the XANES change if the geometric arrangement of the first-shell atoms varies while N_1, R_1, and K_B are kept intact. This is illustrated in Fig. 8, where we display calculated spectra for four (of the total of six) different first-shell types for $N_1 = 4$, $R_1 = 2.2$ Å, and $K_B = 4$. It can be seen that when going from one first-shell type to another, no dramatic changes in the configurationally averaged spectra occur. Nevertheless, for some geometry types, a visible shoulder on the high-energy side of the main peak appears around ~ 35–40 eV, which does not have an experimental counterpart (second and third curves from the bottom of Fig. 8). On the other hand, this shoulder is totally absent in the uppermost and lowermost theoretical graphs. The two undisplayed spectra fall somewhere between these extreme cases. It seems thus that first-shell geometries with larger deviations from a central symmetry perform better than the more symmetric ones. Note finally that absence of a strong dependence of the theoretical XANES on the first-shell geometry suggests that by restricting ourselves to the cubic model alone we do not seriously harm the generality of our conclusions.

Given the fact that the nearest distance between two silver atoms in silver borate crystals is ~ 3 Å (cf. Refs. 56, 57), an evident question arises whether including some Ag atoms into the second shell of our model would not change the overall picture. To check this possibility, we performed another set of calculations for structural models generated in

the same way as above, except that the outermost atom of the cluster was always silver. We found that adding distant Ag atoms produces no significant changes in the calculated spectra; the variations of the XANES curves were less than 5% (we do not show those curves for brevity). We infer, therefore, that Ag K edge XANES of $Ag_2O \cdot nB_2O_3$ glasses is not particularly sensitive to either presence or absence of few silver atoms at "crystallographic" Ag-Ag distances.

We stop our analysis of cube-based models at this point. Obviously a number of other questions arise, such as how sensitive are the calculated spectra towards the *ad hoc* chosen borders of the second shell at 2.5 and 3.0 Å or what happens if more than just eight neighboring atoms are considered. However, our cubic model is only a qualitative one by its nature, so it would not make much sense to make it more "precise." The limited information we obtained is nevertheless worthy: the trends we found in the calculated spectra if N_1, R_1, or K_B are being varied remain valid under quite universal conditions.

3. Influence of various degrees of disorder

The relative independence of the calculated XANES on the arrangement of the first-shell atoms, as displayed in Fig. 8, suggests that a further randomization of our test clusters may be compatible with experiment. Therefore we investigate in this section to what extent does introducing various degrees of randomness affect the calculated Ag spectra. The cube-based structural models explored in Sec. V B 2 include some disorder through averaging over all the configurations which are generated by distributing the available radial distances and chemical types among the second-shell atoms. The directions of the Ag-(O,B) bonds have been, however, fixed (they coincide with the cube diagonals, cf. Fig. 5). By selectively relaxing the restrictions imposed on the angular and/or radial coordinates of first- and second-shell atoms, randomness can be introduced in a controlled manner.

The first step represents relaxing the condition of predefined Ag-(O,B) bond directions for the second-shell atoms. The appropriates tructural model thus can be described as follows: each configuration shares the same rigid first-shell geometry, the radial distances of their second-shell atoms span equidistantly the interval 2.5–3.0 Å as in Sec. V B 2 and the angular coordinates of the second-shell atoms are generated at random. This way of generating test clusters may be called "angular randomization in the second shell." The next logical step is to include "radial randomization" in the second shell on top of the angular randomization. The simplest way to achieve this is to generate the radial distances between the central Ag and the second-shell atoms randomly as uniform deviates (in our case these distances are uniformly distributed in the interval 2.5–3.0 Å). Finally, the positions of first-shell atoms can be randomized as well: first angularly, and then both angularly and radially, in the same way as it has been done for the second-shell atoms. Note that even if both angular and radial randomizations are included in the first as well as in the second shell, one still does not have a complete disorder—the two shells are, namely, still well separated as their radial distances are generated within different intervals, and the first-shell atoms are oxygens
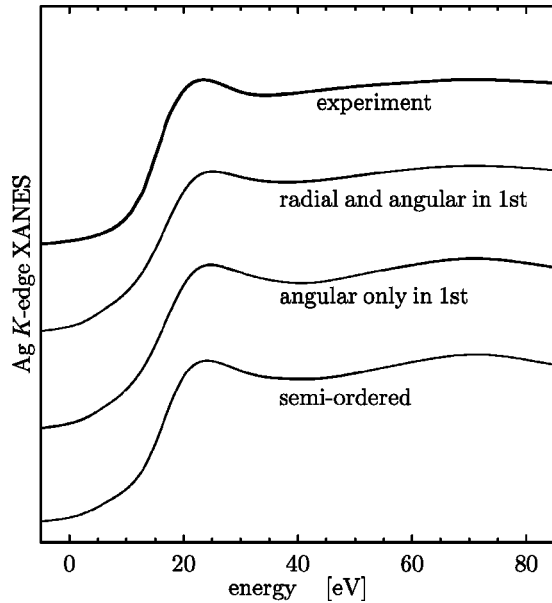
FIG. 9. Comparing effects of various degrees of geometry randomization on averaged XANES spectra. The lowermost curve stands for a semiordered case ($N_1=4$, $R_1=2.2$ Å, $K_B=4$), the second curve from the bottom stands for angular and radial randomization in the second shell plus an angular-only randomization in the first shell, and the third curve displays results for an angular and radial randomization in the first as well as in the second shells. The experimental spectrum of $Ag_2O \cdot 2B_2O_3$ glass is drawn in the top.

FIG. 10. Effect of varying the number of first-shell atoms N_1 for models with angular and radial randomization in both shells. The mean first-shell radial distance is $R_1=2.2$ Å and there are $K_B=4$ borons in each cluster. Experimental spectrum corresponds to the $Ag_2O \cdot 2B_2O_3$ glass. A quantitative evaluation is shown in Table III.

while the second-shell atoms may be both oxygens and borons (their ratio is fixed by K_B). For each of the randomization modes, the corresponding XANES spectrum has to be evaluated as an average over many configurations, as described above. In this work, we used 500 clusters for each randomized model so that a uniform distribution of our configurations is guaranteed. We found that using only a hundred configurations would be sufficient as well. However, note that these configurations stand here as mere representations of the uniform distribution of relevant geometric parameters.

The Ag K edge XANES spectra of models with various degrees of randomization are compared one with another in Fig. 9. We chose the $N_1=4$, $R_1=2.2$ Å, $K_B=4$ cubelike model with the same first-shell geometry as shown by the inset of Fig. 6 as our starting point. The first-shell radial distances were generated so that they fall into the interval 2.0–2.4 Å, so that the original nearest Ag-O distance of $R_1=2.2$ Å remains to be the middle value. The lowermost curve in Fig. 9 shows the spectrum of the original semiordered model, prior to any randomization. The second from the bottom curve stands for the spectrum of the model with both angular and radial randomization in the *second shell* and with angular only randomization in the *first shell* (spectra for models with randomization restricted just to the second shell nearly coincide with this curve so we do not show them here). The third from the bottom curve represents the spectrum of a model with angular and radial randomization in both shells. The experimental spectrum of $Ag_2O \cdot 2B_2O_3$ glass is shown at the top.

It follows from Fig. 9 that randomization does not change the averaged XANES essentially; the relatively good agreement between theory and experiment for the semiordered model is thus not spoilt. Most significant changes occur along this series if the radial randomization of the first shell is switched on at the uppermost theoretical curve. In that case, the theoretical spectrum resembles the experiment better than models with less randomization (the second spectral peak and the valley between the peaks get more flat while the first peak remains relatively sharp). So we conclude that some kind of radial smearing will probably be present already at the first-shell level. Even the semiordered model, namely, contains some radial blurring already—cf. Fig. 6 and the accompanying text.

Our results do not necessarily imply that the local neighborhood around Ag in silver borate glasses has to be random. Let us recall that some models with an angularly well-ordered first shell (explored in Sec. V B 2) also lead to quite a good reproduction of the experimental XANES. Rather, it appears that the more specific details of the local structure—such as angular distribution of the first-shell atoms—do not get revealed in the Ag K edge XANES. This means, on the one hand, that the information we can obtain is only a limited one. On the other hand, it suggests that the limited conclusions that can be drawn from our data are quite robust and general.

4. Trends in XANES of disordered models

We demonstrated in the preceding section that including randomization does not considerably affect the averaged

TABLE III. The R^2 factor and the difference between theoretical and experimental main peaks separations for a randomized model with varying the number of first-shell atoms N_1 (spectra displayed in Fig. 10).

| N_1 | $Ag_2O \cdot 2B_2O_3$ | | $Ag_2O \cdot 4B_2O_3$ | |
	R^2	Δ_{peaks} (eV)	R^2	Δ_{peaks} (eV)
2	0.58	4.4	1.21	6.8
3	0.50	0.3	1.16	2.7
4	0.39	-0.9	1.02	1.5
5	0.69	-2.4	1.49	0.0
6	0.93	-4.0	1.83	-1.6

XANES. In this part we will check whether the general trends of the calculated spectra explored in Sec. V B 2 for semiordered models remain valid for randomized models as well. In that way, namely, a more robust case could be presented for our earlier conclusion that models with $N_1 \sim 4$, $R_1 \sim 2.2$ Å, and $K_B \sim 4$ are preferred by experimental spectra of $Ag_2O \cdot nB_2O_3$ glasses. We focus on models with both angular and radial randomization applied for both shells. As in the preceding section, radial distances of the first-shell atoms deviate from the middle value R_1 by at most 0.2 Å and the radial distances of the second-shell atoms are uniformly distributed between 2.5 and 3.0 Å. The R^2 and Δ_{peaks} values are shown here as well (cf. Sec. V A), in order to offer a quantitative assessment of the effect of varying selected structural parameters.

The effect of varying the number of first-shell atoms N_1 is investigated in Fig. 10. The number of first-shell atoms varies from 2 to 6, while the mean first-shell radial distance $R_1 = 2.2$ Å and the number of boron atoms $K_B = 4$ are kept fixed. The first shell is preferentially occupied by oxygens, only for $N_1 > 4$ there are also $(N_1 - 4)$ borons present in the first shell. It is clear from the calculated curves that the first maximum is too small for models with low N_1 and too broad for models with high N_1. The middle values around $N_1 \approx 3$ or 4 seem to be most plausible.

The effect of varying the mean first-shell distance R_1 for fixed $N_1 = 4$ and $K_B = 4$ is investigated in Fig. 11. The separation between the two main spectral peaks systematically decreases if R_1 is increased, indicating that $Ag_2O \cdot nB_2O_3$ glasses with smaller n might have shorter nearest-neighbor Ag-O distances than glasses with larger n (cf. Fig. 1 to see all the experimental spectra). The best overall agreement with experiment is obtained for $R_1 = 2.2$ Å (peaks separation 45.6 eV), similarly as was the case for semiordered models in Sec. V B 2.

Finally, in Fig. 12, we study the influence of the number of borons in the cluster, keeping the number of first-shell atoms $N_1 = 4$ and their mean distance $R_1 = 2.2$ Å fixed while varying K_B. The first shell is filled preferentially with oxygens and only if their number $(8 - K_B)$ is lower than $N_1 = 4$, the borons enter the first shell to top it up. One can see from Fig. 12 that at least $K_B = 2$ borons are needed to generate the first spectral peak properly, which is a strong indication that no reliable structural model can be built if the borons are omitted. On the other hand, there appears to be only a mild
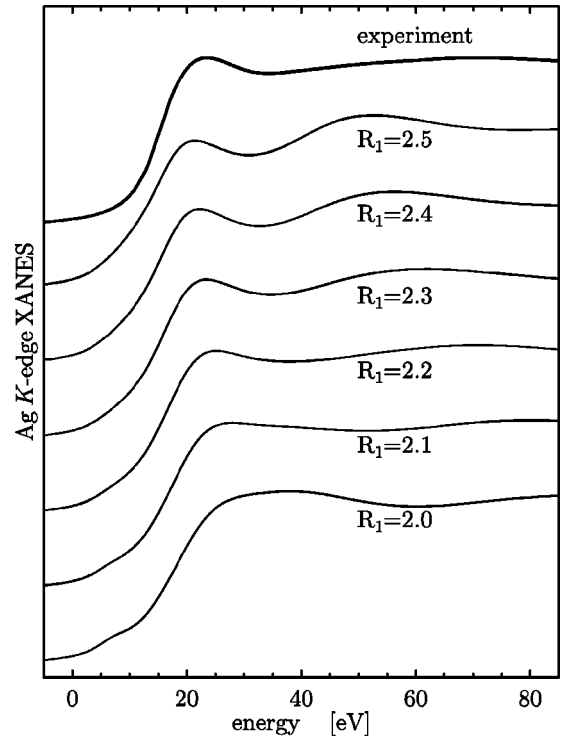
FIG. 11. Effect of varying the mean first-shell distance R_1 for models with angular and radial randomization in both shells. The number of first-shell atoms is $N_1 = 4$ and there are $K_B = 4$ borons in each cluster. A quantitative evaluation is shown in Table IV.

K_B dependence of the calculated spectra for $K_B \geq 3$. The separation of the two main peaks decreases uniformly with K_B, from 46.4 eV for $K_B = 2$ to 42.2 eV for $K_B = 6$. This is a plausible result: experiment shows that spectra of compositions with larger n (hence also larger concentration of B atoms) exhibit smaller separations between the peaks than compositions with smaller n. We conclude this section by observing that the analysis of the *disordered* models implies similar conclusions as the analysis of the semiordered cubic model: i.e., the silver atoms are coordinated by about four oxygens at the distance $R_1 = 2.2$–2.3 Å, surrounded by further shell of about the same or higher number of atoms, mainly borons, distributed in the radially blurred second shell (tentatively somewhere between 2.5 and 3.0 Å).

TABLE IV. The R^2 factor and the difference between theoretical and experimental main peaks separations for a randomized model with varying the mean first-shell distance R_1 (spectra displayed in Fig. 11).

| R_1 (Å) | $Ag_2O \cdot 2B_2O_3$ | | $Ag_2O \cdot 4B_2O_3$ | |
	R^2	Δ_{peaks} (eV)	R^2	Δ_{peaks} (eV)
2.0	10.12	4.8	13.03	7.2
2.1	1.20	5.7	2.37	8.1
2.2	0.39	-0.9	1.02	1.5
2.3	0.34	-7.9	0.72	-5.5
2.4	0.54	-12.6	0.79	-10.2
2.5	0.78	-15.3	0.94	-12.9
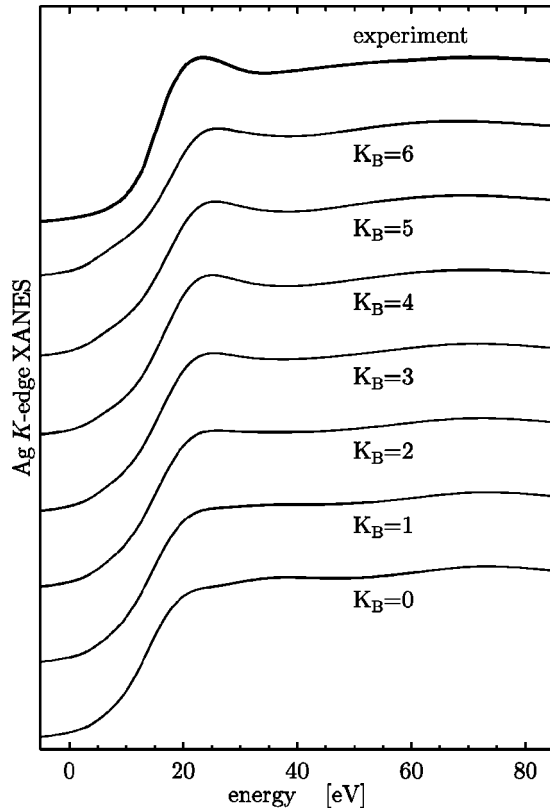
FIG. 12. Effect of varying the number of borons in the cluster K_B for models with angular and radial randomization in both shells. The number of first-shell atoms is $N_1 = 4$ and the mean first-shell radial distance is $R_1 = 2.2$ Å for each model of this sequence. A quantitative evaluation is shown in Table V.

TABLE V. The R^2 factor and the difference between theoretical and experimental main peaks separations for a randomized model with varying the number of borons in the cluster K_B (spectra displayed in Fig. 12).

K_B	$Ag_2O \cdot 2B_2O_3$		$Ag_2O \cdot 4B_2O_3$	
	R^2	Δ_{peaks} (eV)	R^2	Δ_{peaks} (eV)
0	12.61	-11.2	15.33	-8.8
1	13.89	-12.0	16.71	-9.6
2	0.77	-0.1	1.73	2.3
3	0.51	-0.3	1.28	2.1
4	0.39	-0.9	1.02	1.5
5	0.73	-2.7	1.50	-0.3
6	1.10	-4.3	1.96	-1.9

VI. DISCUSSION

The evident impossibility to obtain a satisfactory single-configuration description of the experimental XANES spectra of $Ag_2O \cdot nB_2O_3$ borate glasses forced us to adopt a different approach to the analysis of XANES of amorphous system, different from the more intuitive best-fit approach.[5] Good results have been obtained by a systematic exploration of the changes of the calculated spectra which occur if well identified basic structural characteristics are varied. This procedure represents an alternative to the conceptually more simple best-fit method in situations where its application would lead to ambiguous results[36] due to a vast number of structural parameters that have to be fitted, as is the present case. Our study deals solely with analyzing the near-edge region; for a more complete structural information, EXAFS analysis ought to be performed whenever possible, for which our procedure certainly cannot be a substitute. Rather, our results could serve as a guide and inspiration for a more quantitative investigation based on examining x-ray absorption spectra both in the XANES and in the EXAFS regions. Note also that some preceding information gained from preliminary EXAFS study[17] and from neutron scattering experiments[10] was in fact needed so that a reasonable guess of the starting point of our analysis could be made in Secs. V B 1 and V B 2.

One is naturally confronted with the question of robustness, completeness, and reliability of our results. By focusing on the cubic and random models, we necessarily left out plenty of other conceivable geometries. One could contemplate using different numbers of atoms in the cluster, modifying the boundaries of the second shell, and so on. However, the amount of information which can be extracted from the Ag K edge XANES of silver borate glasses is in any case limited (recall the low sensitivity of averaged spectra towards the arrangement of the first-shell atoms). Therefore, a further widening of the classes of models we investigate would hardly lead to any really new findings. A truly complete and unique solution apparently cannot be obtained for a structure of a glass for which a single-configuration approach fails. At the same time, the *trends* in the calculated spectra which we uncovered are quite general ones, valid for both semiordered and randomized situations, hence one can trust that the information we get, even if limited, is quite reliable and not just specific to the kind of models we employed. The information we obtained in this way could serve as a guide for building more refined structural models of silver borate glasses in the future.

We found that plausible models of the Ag neighborhood are characterized by the presence of two radially smeared coordination shells. The first shell is formed by about four oxygens at a mean distance of $R_1 \approx 2.2$ Å. Compositions with large n will have smaller R_1 than compositions with smaller n. The second shell contains four or more atoms, predominantly borons, and may stretch from ~ 2.5 Å to approximately 3.0 Å (or further). Structural models for compositions with larger n favor higher proportion of borons in the Ag neighborhood than models for compositions with small n. Presence of few Ag atoms at around 3.0 Å from the central atom is compatible with our data though not necessary for explaining them.

When interpreting these results, one has to bear in mind that our conclusions about the structural characteristics concern their *mean values*; the experimental Ag spectrum is in fact a superposition of several spectra which correspond to photoabsorbing silver atoms being in maybe quite different local coordinations. It is thus clear that randomization should be included in realistic models of silver borate glasses. In particular, the radial smearing of the nearest shell is essential for flattening of the second experimental XANES peak (cf.

Fig. 9). The second shell has to be radially blurred as well; otherwise one gets redundant oscillations in the region between the two main peaks (cf. Fig. 6). The shape of the first spectral peak, on the other hand, is not significantly affected by the structural randomization. Randomization restricted to the angular coordinates only does not have a profound influence on the calculated spectra either.

Details of the geometric arrangement of the nearest neighbors have little influence on the configurationally averaged spectra if some disorder in the second shell is introduced (cf. Fig. 8). This result is consistent with the multiconfiguration study of silica by Levelut *et al.*,[35] who discovered that a broad distribution of bond angles and distances within the set of test clusters leads to a lower sensitivity of XANES to small differences between various (multiconfiguration) structural models. It thus appears that inaccessibility of some finer structural details through XANES analysis may a general feature of all systems which have to be described by a multiconfiguration approach.

One can speculate whether there is an intuitive physical reason for the fact that the local structure around Ag in silver borate glasses cannot be described by a single geometric configuration. The tentative explanation for the different ways of describing amorphous germanium or metal silicates on the one hand (where a single-configuration approach works fine) (Refs. 25–27) and $Ag_2O \cdot nB_2O_3$ glasses on the other hand may rest in the different roles played by the photoabsorbing atoms in the formation of the structural network of these materials: Ge in amorphous germanium as well as Ti, Al, and Si in metal silicates are network *formers* while Ag in silver borates is just a network *modifier*, being not directly incorporated into the B-O chains. Oxygen atoms, through which the silver atoms bind to the B-O chains, occur in many nonequivalent positions (even in $Ag_2O \cdot nB_2O_3$ crystals), hence one can anticipate that there will be plentiful nonequivalent Ag sites in silver borate glasses, making thus a single-configuration approach impractical.

Based on this intuition, one would expect that other chemically similar systems would also be prone rather to a multiconfiguration than to a single-configuration description. An analysis of a Cu K edge XANES in silicate glasses containing Cu^+ ions, which ought to have similar properties as Ag ions, was performed by Maurizio *et al.*[61] within the single-configuration framework only. However, the agreement between the theoretical single-configuration model XANES and the experiment was not found to be especially good in that work. Our results suggest that a multiconfiguration approach might be more suitable for analyzing XANES of this type of materials well.

It is conceivable that the low coordination number of Ag deduced from earlier EXAFS studies of $Ag_2O \cdot nB_2O_3$ glasses[17] results from the fact that the signal from highly coordinated Ag atoms is suppressed by a strong disorder around those sites while some other low coordinated Ag atoms may have a more ordered neighborhood and contribute thus dominantly to the measured EXAFS spectrum. On the other hand, the XANES signal need not be so strongly damped by the disorder because of a lower photoelectron energy (note that the damping grows exponentially with en-

ergy in the simple description based on the Debye-Waller factors). Therefore, the contribution from Ag atoms with a higher coordination may get revealed differently in XANES or in EXAFS. Note that Farges *et al.*[42] also observed that disorder associated with more distant neighbors affects XANES less than EXAFS.

VII. CONCLUSIONS

A detailed comparison of experimental XANES spectra of $Ag_2O \cdot nB_2O_3$ glasses with the theoretical spectra of known crystallographic sites in borate crystals has been presented. The Ag K edge XANES spectra of silver borate glasses cannot be described on the basis of a single-configuration framework. A reasonable agreement between theory and experiment can be achieved only if large structural disorder is incorporated via the multiconfigurational approach.

In order to interpret the XANES of disordered systems where a single-configuration approach fails, we suggest an alternative approach to the conventional best-fit method. This method tries to reproduce the experiment by averaging over many configurations generated assuming a distribution of possible local structures. The parameters characterizing these configurations (radial distances, coordination numbers, and type of nearest and next nearest neighbors) are singularly varied and analyzed.

Although slower and more cumbersome than the conventional best-fit method, this approach allows us to check the actual influence of each parameter on the configurationally averaged spectrum. The overall trends observed in the calculated spectra of silver borate glasses when some basic structural characteristics were varied seem to be valid under quite general conditions. The critical analysis of such trends may result in a more widely applicable method for extracting structural information from XANES spectra of amorphous systems.

It appears that the structural analysis at the K edge of Ag in silver borate glasses is particularly complex due to a large number of oxygens and borons surrounding Ag at a distance $\lesssim 3$ Å. This is a general situation which is present in glasses, especially in the environment of modifier species which tend to assume multiple structural configurations. In these cases we have shown that XANES analysis may be a very useful tool to select the most probable local configurations. A combined quantitative analysis of both XANES and EXAFS signals is highly desirable, at this point. Work is in progress to optimize a numerical procedure able to combine the results of theoretical simulations of XANES and EXAFS (and, possibly, diffraction techniques), in a reasonable computational time.

[1] *X-ray Absorption: Principles, Applications, Techniques of EXAFS, SEXAFS, and XANES*, edited by D.C. Koningsberger and R. Prins (Wiley, New York, 1998); J. Stöhr, *NEXAFS Spectroscopy* (Springer, Berlin, 1990).

[2] A.L. Ankudinov, B. Ravel, J.J. Rehr, and S.D. Conradson, Phys. Rev. B **58**, 7565 (1998).

[3] Y. Joly, Phys. Rev. B **63**, 125120 (2001).

[4] M. Benfatto and S. Della Longa, J. Synchrotron Radiat. **8**, 1087 (2001); S. Della Longa, A. Arcovito, M. Girasole, J.L. Hazemann, and M. Benfatto, Phys. Rev. Lett. **87**, 155501 (2001).

[5] M. Benfatto, S. Della Longa, and C.R. Natoli, J. Synchrotron Radiat. **10**, 51 (2003).

[6] S.A. Feller, Phys. Chem. Glasses **41**, 211 (2000).

[7] T. Minami, J. Non-Cryst. Solids **73**, 273 (1975).

[8] G. Calas, L. Cormier, L. Galoisy, and P. Jollivet, C.R. Acad. Sci., Ser. IIc: Chim **5**, 831 (2002).

[9] C.P. Varsamis, E.I. Kamitsos, and G.D. Chryssikos, Phys. Rev. B **60**, 3885 (1999).

[10] J. Swenson, L. Börjesson, and W.S. Howells, J. Phys.: Condens. Matter **11**, 9275 (1999).

[11] L. Červinka, J. Bergerová, A. Dalmaso, and F. Rocca, J. Non-Cryst. Solids **232-234**, 627 (1998).

[12] G. Dalba, P. Fornasini, F. Rocca, and E. Burattini, J. Phys. (Paris), Colloq. **47** (C8), 749 (1986).

[13] G. Dalba, P. Fornasini, F. Rocca, E. Bernieri, E. Burattini, and S. Mobilio, J. Non-Cryst. Solids **91**, 153 (1987).

[14] G. Dalba, P. Fornasini, and F. Rocca, J. Non-Cryst. Solids **123**, 310 (1990).

[15] F. Rocca, G. Dalba, P. Fornasini, and A. Tomasi, Solid State Ionics **53-56**, 1253 (1992).

[16] F. Rocca, J. Phys. IV **2**, 97 (1992).

[17] F. Rocca, G. Dalba, P. Fornasini, and F. Monti, in *Proceedings of Second International Conference on Borate Glasses, Crystals and Melts, Abington, 1996*, edited by A. C. Wright, S. A. Feller, and A. C. Hannon (Society of Glass Technology, Sheffield, 1997), p. 295.

[18] J. Swenson, L. Borjesson, R.L. McGreevy, and W.S. Howells, Phys. Rev. B **55**, 11 236 (1997).

[19] J. Swenson, L. Borjesson, and W.S. Howells, Phys. Rev. B **52**, 9310 (1995).

[20] G. Dalba, P. Fornasini, F. Rocca, and F. Monti, J. Non-Cryst. Solids **293-295**, 93 (2001).

[21] G. Dalba, P. Fornasini, R. Grisenti, N. Daldosso, S.A. Beccara, A. Sanson, F. Rocca, F. Monti, and A. Kuzmin, Phys. Chem. Glasses **44**, 75 (2003).

[22] G. Dalba, P. Fornasini, A. Kuzmin, F. Monti, A. Sanson, O. Šipr, and F. Rocca, Physica Scripta (to be published).

[23] A. Kuzmin, J. Phys. IV **7**, 213 (1997).

[24] J.J. Rehr and R.C. Albers, Rev. Mod. Phys. **72**, 621 (2000).

[25] O. Yanagisawa, T. Fujikawa, and S. Naoe, Jpn. J. Appl. Phys. **37**, 230 (1998).

[26] F. Farges, G.E. Brown, Jr., A. Navrotsky, H. Gan, and J.J. Rehr, Geochim. Cosmochim. Acta **60**, 3039 (1996).

[27] Z. Wu, C. Romano, A. Marcelli, A. Mottana, G. Cibin, G. Della Ventura, G. Giuli, P. Courtial, and D.B. Dingwell, Phys. Rev. B **60**, 9216 (1999).

[28] A.N. Mansour, A. Marcelli, G. Cibin, G. Yalovega, T. Sevastyanova, and A.V. Soldatov, Phys. Rev. B **65**, 134207 (2002).

[29] P. Kizler, P. Lamparter, and S. Steeb, Z. Naturforsch., A: Phys. Sci. **44a**, 189 (1989).

[30] P. Kizler, Phys. Rev. Lett. **67**, 3555 (1991).

[31] P. Kizler, Phys. Rev. B **48**, 12 488 (1993).

[32] P.J. Merkling, A. Muñoz-Páez, R.R. Pappalardo, and E. Sánchez Marcos, Phys. Rev. B **64**, 092201 (2001).

[33] G.R. Harp, D.K. Saldin, and B.P. Tonner, J. Phys.: Condens. Matter **5**, 5377 (1993).

[34] J. Chaboy, M. Benfatto, and I. Davoli, Phys. Rev. B **52**, 10 014 (1995).

[35] C. Levelut, D. Cabaret, M. Benoit, P. Jund, and A.-M. Flank, J. Non-Cryst. Solids **293-295**, 100 (2001).

[36] P. Kizler, P. Lamparter, and S. Steeb, Physica B **158**, 392 (1989).

[37] J. Guo, D.E. Ellis, E. Alp, L. Soderholm, and G.K. Shenoy, Phys. Rev. B **39**, 6125 (1989).

[38] F. Farges, G.E. Brown, Jr., and J.J. Rehr, Phys. Rev. B **56**, 1809 (1997).

[39] R.V. Vedrinskii, V.L. Kraizman, A.A. Novakovich, Ph.V. Demekhin, and S.V. Urazhdin, J. Phys.: Condens. Matter **10**, 9561 (1998).

[40] O. Šipr, A. Šimunek, S. Bocharov, Th. Kirchner, and G. Dräger, Phys. Rev. B **60**, 14 115 (1999).

[41] O. Šipr, Phys. Rev. B **65**, 205115 (2002).

[42] F. Farges, G.E. Brown, Jr., and J.J. Rehr, Geochim. Cosmochim. Acta **60**, 3023 (1996).

[43] L.A. Bugaev, A.P. Sokolenko, H.V. Dmitrienko, and A.-M. Flank, Phys. Rev. B **65**, 024105 (2001).

[44] F.Al Shamma, M. Abbate, and J.C. Fuggle, in *Unoccupied Electron States*, edited by J. C. Fuggle and J. E. Inglesfield (Springer, Berlin, 1992), p. 347.

[45] D. D. Vvedensky, in *Unoccupied Electron States*, edited by J. C. Fuggle and J. E. Inglesfield (Springer, Berlin, 1992), p. 139; C.R. Natoli, M. Benfatto, S. Della Longa, and K. Hatada, J. Synchrotron Radiat. **10**, 26 (2003).

[46] D.D. Vvedensky, D.K. Saldin, and J.B. Pendry, Comput. Phys. Commun. **40**, 421 (1986).

[47] O. Šipr, computer code RSMS (Institute of Physics AS CR, Prague, 1996).

[48] M. Cook and D.A. Case, computer code XASCF (Quantum Chemistry Program Exchange, Indiana University, Bloomington, Indiana, 1980).

[49] O. Šipr, F. Rocca, and G. Dalba, J. Synchrotron Radiat. **6**, 770 (1999).

[50] See, e.g., W.E. Pickett, Comput. Phys. Commun. **9**, 115 (1989).

[51] W. Kohn and L.J. Sham, Phys. Rev. **140**, A1133 (1965).

[52] J. Chaboy and S. Quartieri, Phys. Rev. B **52**, 6349 (1995).

[53] A.L. Ankudinov and J.J. Rehr, J. Phys. IV **7**, 121 (1997).

[54] W. Speier, R. Zeller, and J.C. Fuggle, Phys. Rev. B **32**, 3597 (1985).

[55] P. D'Angelo, M. Benfatto, S. Della Longa, and N.V. Pavel, Phys. Rev. B **66**, 064209 (2002).

[56] M. Jansen and W. Scheld, Z. Anorg. Allg. Chem. **477**, 85 (1981).

[57] G. Brachtel and M. Jansen, Z. Anorg. Allg. Chem. **478**, 13 (1981).

[58] J. Krogh-Moe, Acta Crystallogr. **18**, 77 (1965).

[59] S.F. Radaev, L.A. Muradyan, L.F. Malakhova, Y.A. Burak, and V.I. Simonov, Sov. Phys. Crystallogr. **34**, 842 (1989).

[60] J. Krogh-Moe, Acta Crystallogr., Sect. B: Struct. Crystallogr. Cryst. Chem. **30**, 747 (1974); J. Krogh-Moe, *ibid.* **28**, 1571 (1972).

[61] C. Maurizio, F. d'Acapito, M. Benfatto, S. Mobilio, E. Cattaruzza, and F. Gonella, Eur. Phys. J. B **14**, 211 (2000).